Acta Crystallographica Section D
Biological Crystallography
ISSN 0907-4449

A rapid method for assessing lipid:protein and detergent:protein ratios in membrane-protein crystallization

Corrie J. B. daCosta and John E. Baenziger*

Department of Biochemistry, Microbiology and Immunology, University of Ottawa, 451 Smyth Road, Ottawa, Ontario K1H 8M5, Canada

Correspondence e-mail: jebaenz@uottawa.ca

Received 17 July 2002
Accepted 18 October 2002

A simple procedure for rapidly measuring lipid:protein ratios and detergent concentrations at different stages of the solubilization, purification and crystallization of membrane proteins has been developed. Fourier-transform infrared spectra recorded from 10 µl aliquots of solution using a single-bounce diamond-attenuated total reflectance apparatus exhibit characteristic bands arising from the vibrations of lipid, protein and detergent. Lipid:protein molar ratios as low as 5:1 (for a protein with a molecular weight of 300 kDa) are determined by comparing the ratio of the integrated intensity of the lipid ester carbonyl band near 1740 cm^{-1} with the protein amide I band near 1650 cm^{-1}. Detergent concentrations at levels well below the critical micellar concentration of most detergents are determined by comparing the integrated intensities of the detergent vibrations, particularly in the 1200–1000 cm^{-1} region, with a standard curve. Protein amide I band-shape analysis provides insight into the effects of detergents on protein secondary structure. The importance of monitoring detergent concentration changes during simple procedures, such as the concentration of a membrane protein by ultrafiltration, is demonstrated. This analytical tool has been used to rapidly establish protocols for minimizing lipid and detergent levels in solubilized membrane-protein samples.

1. Introduction

The structural characterization of integral membrane proteins by X-ray crystallography has lagged far behind that of soluble proteins, mainly because of the difficulties associated with the formation of membrane-protein crystals (Garavito & Picot, 1990; Garavito *et al.*, 1996; Kuhlbrandt, 1988; Ostermeier & Michel, 1997; Rosenbusch *et al.*, 2001). Membrane proteins are difficult to crystallize because they have large hydrophobic surfaces that render them insoluble in aqueous solution. While insolubility can usually be overcome by removing the proteins from their membrane environment with the use of detergents, finding suitable conditions that lead to the formation of stable protein–detergent or protein–lipid–detergent complexes for crystallization can be a daunting task.

Both the concentration and physical properties of the detergent are important factors that affect the solubilization of membrane proteins and thus ultimately their crystallization (Le Maire *et al.*, 2000). Sufficient detergent must be present to first remove the protein from its membrane environment and then to prevent the formation of non-specific protein–protein aggregates or precipitates. Excessive detergent, however, can lead to both protein denaturation and the formation of protein-free micelles which may interfere with crystal forma-

© 2003 International Union of Crystallography
Printed in Denmark – all rights reserved

tion. The size of the detergent belt surrounding a membrane protein, which depends on the physical properties of the detergent, can also hinder the formation of protein–protein contacts in a growing crystal (Pebay-Peyroula *et al.*, 1995; Roth *et al.*, 1989). Furthermore, detergent phase phenomena, which are highly dependent on detergent concentration, may have important implications in crystal nucleation (Hitscherich *et al.*, 2000; Loll *et al.*, 2001). Although membrane proteins are likely to be most stable in the presence of minimal detergent, each protein is likely to have a select detergent and detergent concentration range under which crystallization is favourable.

The level of endogenous lipid in a solubilized membrane-protein sample can also influence the structural integrity and thus the crystallizability of a protein. Some proteins, such as the light-harvesting complex II, crystallize in the presence of a number of specifically bound lipids, whereas others, such as the porins, only crystallize in minimal lipid (Garavito & Rosenbusch, 1986; Kuhlbrandt, 1988). Excess lipid can form protein-free lipid/detergent micelles that interfere with crystal growth and may also increase the effective size of the detergent belt surrounding the protein's transmembrane domain, thus making crystal contacts sterically unfavourable. As with detergents, membrane-protein crystallization is likely to be optimal under a select range of lipid:protein ratios.

An initial step in the crystallization of a membrane protein requires an understanding of how the lipid:protein and detergent:protein ratios influence both the structural stability and solubility of the protein. Understanding these correlations, however, is hampered because there are no simple rapid methods available for assessing the levels of lipid and detergent in crystallization solutions. Here, we report on the use of Fourier-transform infrared (FTIR) spectroscopy to monitor lipid:protein ratios and detergent concentrations in membrane-protein crystallization solutions. We have used a commercially available single-bounce diamond-attenuated total reflectance accessory to rapidly record spectra from detergent-solubilized membrane-protein solutions using volumes as low as 5–10 µl per sample. This approach can be used to quickly and accurately assess lipid:protein ratios and detergent concentrations, as well as to give an indication of protein structural integrity at all stages of the crystallization process.

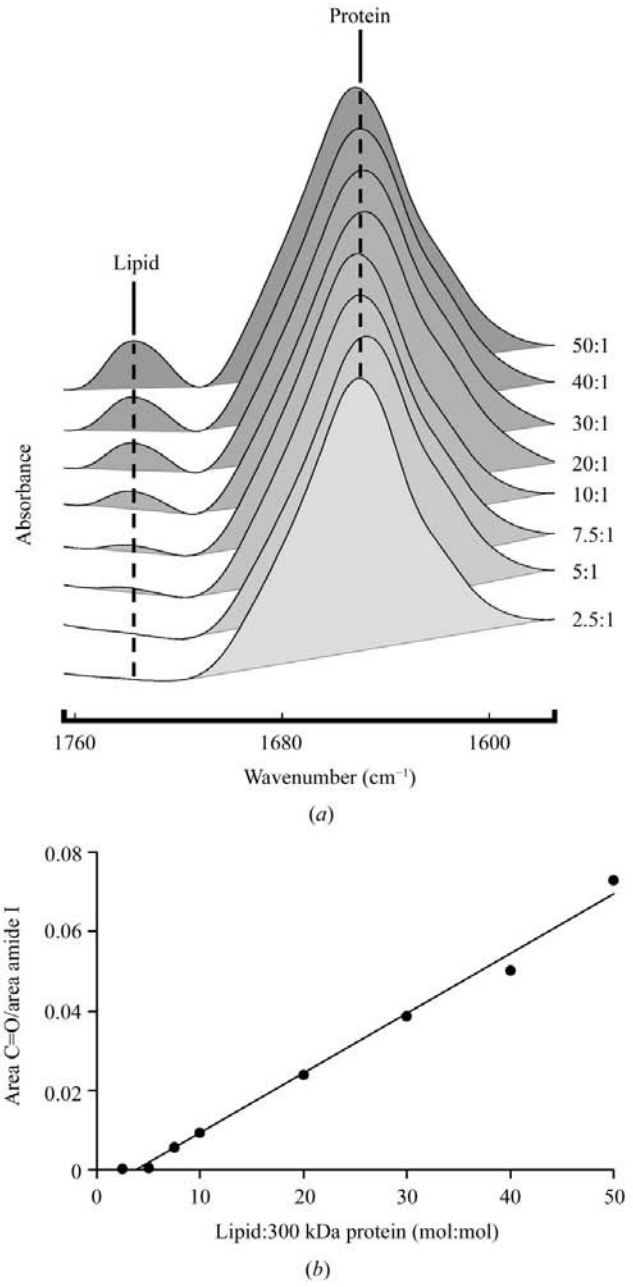

Figure 1
(*a*) Dry FTIR spectra of lysozyme and 1-palmitoyl-2-oleoyl-*sn*-glycero-3-phosphocholine (POPC) at different lipid:protein ratios. The lipid:protein ratio (mol:mol) for a 300 kDa protein is shown to the right of each spectrum. The shading denotes the areas for both lipid and protein that were integrated to calculate the standard curve. (*b*) Lipid–protein standard curve calculated from the spectra in (*a*).

2. Materials and methods

2.1. FTIR

Spectra were acquired using a single-reflection attenuated total reflectance (ATR) apparatus with a diamond internal reflection element (Specac, Kent, England or ASi/SensIR, Warrington, England). The ATR apparatus was installed in either a BioRad FTS-40 or FTS-575c FTIR spectrometer (Randolph, MA, USA). Both spectrometers were equipped with a deuterated tryglycine sulfate (DTGS) detector and were purged with dry air (dew point 373 K) from a Balston (Haverhill, MA, USA) air dryer to minimize spectral contributions from atmospheric water vapour. The temperature at the surface of the diamond IRE was 295–298 K. All figures were prepared with *GPLOTC* (NRC, Ottawa, ON, Canada) and *Microsoft Office 97* (Microsoft).

2.2. Lipid–protein standard curve

Standard solutions with different ratios of 1-palmitoyl-2-oleoyl-*sn*-glycero-3-phosphocholine (POPC; Avanti Polar Lipids, Alabaster, AL, USA) to lysozyme (Sigma, Oakville, ON, Canada) were prepared in 100 m*M* NaCl, 10 m*M* Tris–

HCl pH 7.5, 0.1 m*M* EDTA and 0.02%(*w*/*v*) NaN_3 in H_2O. The final concentration of lysozyme in each standard was 30 mg ml^{-1} (BioRad protein assay, BioRad, Mississauga, ON, Canada). After thorough vortexing, a 10 µl drop of each standard solution was placed on the diamond internal reflection element and dried completely with a stream of N_2 gas (the absorption of ^1H_2O at 3500 cm^{-1} was monitored to ensure complete evaporation). 512 scans at 4 wavenumber resolution were then collected and co-added. For each FTIR spectrum, the area under both the lipid ester carbonyl (1710–1765 cm^{-1}) and the protein amide I (1580–1710 cm^{-1}) bands were determined by drawing a line between the minima on either side of each band and then integrating the area between the line and the spectrum using the data-analysis software *GRAMS* 32 (Galactic Industries, Salem, NH, USA). The areas used in the integration procedure are denoted by the shaded regions in Fig. 1(*a*).

Lipid:protein (mol:mol) ratios were calculated from the relative weights of lipid and protein in each solution assuming a M_r of 760.1 for POPC and a MW of 300 kDa for the protein. The latter is justified because the intensity of the amide I band is proportional to the number of peptide C═O functional groups, regardless of the molecular weight of the protein. A MW of 300 kDa is relevant to studies of the nicotinic acetylcholine receptor (nAChR; see below).

2.3. Detergent standards

All detergent standards were made in 10 m*M* Tris–HCl ^1H_2O pH 7.5. The *n*-octyl-β-D-glucoside (β-OG), *N*-dodecyl-*N*,*N*-dimethyl-3-ammonio-1-propanesulfonate (Zwittergent 3-12) and cholate were from Sigma (Oakville, ON, Canada), while the *n*-decyl-β-D-maltopyranoside (C_{10}M) and octaethylene glycol monotridecyl ether ($C_{12}E_8$) were from Calbiochem (La Jolla, CA, USA).

For the octylglucoside standard curve, a 10 µl drop of each standard was placed on the surface of the diamond ATR. 512 scans at 4 wavenumber resolution were co-added for each spectrum, which took approximately 10.5 min using a DTGS detector. This length of time is ideal in that the drop does not dry out appreciably during spectral acquisition. The number of scans is sufficient to obtain a very high signal-to-noise ratio. Comparable spectra have also been recorded with a mercury cadmium telluride (MCT) detector, which acquires 512 scans in about 1.5 min. Solvent (10 m*M* Tris–HCl ^1H_2O pH 7.5) subtraction was performed with *GRAMS* 32 software so that the region encompassing the detergent bands approximated a flat baseline. The area under the spectra corresponding to the detergent bands (947–1187 cm^{-1}) was integrated (*GRAMS* 32) and plotted against the known octylglucoside concentration (Fig. 3).

2.4. Protein secondary structure

10 µl of 10, 30 and 60 mg ml^{-1} lysozyme (Sigma, Oakville, ON, Canada) in 100 m*M* NaCl, 10 m*M* Tris pH 7.5, 0.1 m*M* EDTA and 0.02%(*w*/*v*) NaN_3 in ^1H_2O was placed on the diamond ATR surface and 512 scans were acquired at 4 wavenumber resolution. For the denatured sample, lysozyme was incubated at 373 K for 20 min prior to spectral acquisition. Aqueous buffer and residual H_2O vapour was subtracted using *GRAMS* 32 software (Reid *et al.*, 1996).

2.5. Ultrafiltration experiment

The nicotinic acetylcholine receptor was affinity purified as described elsewhere (daCosta *et al.*, 2002), except that it was eluted in cholate elution buffer. The eluate was pooled and concentrated at 1000*g* using a 100 kDa molecular-weight cutoff (MWCO) concentrator (Millipore, Ottawa, ON, Canada). Aliquots were removed at 5 min intervals and the nAChR concentration was determined by the BCA protein assay (Pierce). Cholate concentration was determined using FTIR by integrating cholate spectral features (992–1135 cm^{-1}) and comparison with a cholate standard curve (not shown).

3. Results

3.1. FTIR data-acquisition accessories

Our primary goal was to establish a method for measuring both lipid:protein ratios and detergent concentrations in solutions containing detergent-solubilized integral membrane proteins. FTIR spectroscopy, which is sensitive to bond vibrational frequencies, could be used to measure both parameters (Goormaghtigh *et al.*, 1990; Pistorius *et al.*, 1994). FTIR can also be used to investigate protein secondary structure and could thus shed light on how lipid:protein ratios and detergent concentrations influence protein structural stability (He *et al.*, 1991). The problem, however, is that the accessories (either transmission or ATR) commonly used to acquire spectra from biological samples are not amenable to rapid screening of many small aliquots. We required a sampling accessory that allows rapid spectral acquisition from small aliquots at all stages of our sample preparation.

We tested the utility of a diamond ATR microsampling accessory for acquiring spectra from detergent-solubilized membrane-protein samples (Figs. 1, 2, 3 and 4). The advantages of this ATR accessory are the ease of sample preparation and the small sample requirements. 5–10 µl of solution are simply placed on the surface of the ATR accessory and spectra are acquired. The total time for sample preparation and spectral acquisition can be less than 1 min, although longer times were used here to increase the number of scans and thus obtain a higher signal-to-noise ratio. In addition, the diamond ATR crystal is easily cleaned for repeated spectral analyses.

3.2. Lipid:protein ratios

The utility of the ATR accessory for assessing lipid:protein ratios is demonstrated in Fig. 1. Spectra recorded from dried solutions (see §2) containing a constant concentration of the protein lysozyme and increasing levels of the lipid POPC exhibit two main infrared vibrations in the 1760–1550 cm^{-1} region (Fig. 1*a*). The broad amide I band between 1600 and 1700 cm^{-1} arises primarily from the C═O stretching vibration of the polypeptide backbone, whereas the relatively narrow

band between 1700 and 1760 cm^{-1} arises from the C=O stretching vibration of lipid ester carbonyl groups (Jackson & Mantsch, 1995; Mendelsohn & Mantsch, 1986). The relative area of the lipid C=O and amide I band is directly related to the lipid:protein ratio as shown in the standard curve (Fig. 1*b*). Note that the molar lipid:protein ratio has been calculated for a 300 kDa protein (*i.e.* nAChR). As seen in both Figs. 1(*a*) and 1(*b*), the technique can accurately detect lipid:protein ratios down to roughly five molecules of lipid per molecule of 300 kDa protein.

3.3. Detergent concentration

The applicability of the diamond ATR accessory for measuring detergent concentrations in solubilized membrane-protein samples is illustrated in Figs. 2 and 3. Five representative spectra of detergents commonly used in membrane-protein purification and crystallization are compared with the absorption spectra of DPPC and lysozyme in Figs. 2(*a*)–2(*e*). Each detergent exhibits spectral features in the 1200–900 cm^{-1} region that do not overlap with the absorption bands of proteins (Fig. 2*g*). Although lipid does absorb in the 1200–900 cm^{-1} region (Fig. 2*f*), the spectral contributions of lipids are negligible at the lipid:protein ratios normally found in our detergent solubilized membrane-protein samples (usually less than 30:1 mol:mol lipid:protein). In cases with very high lipid and very low detergent, the contributions of lipid can be scaled and subtracted from the spectra in order to quantify the intensities of the detergent bands (not shown).

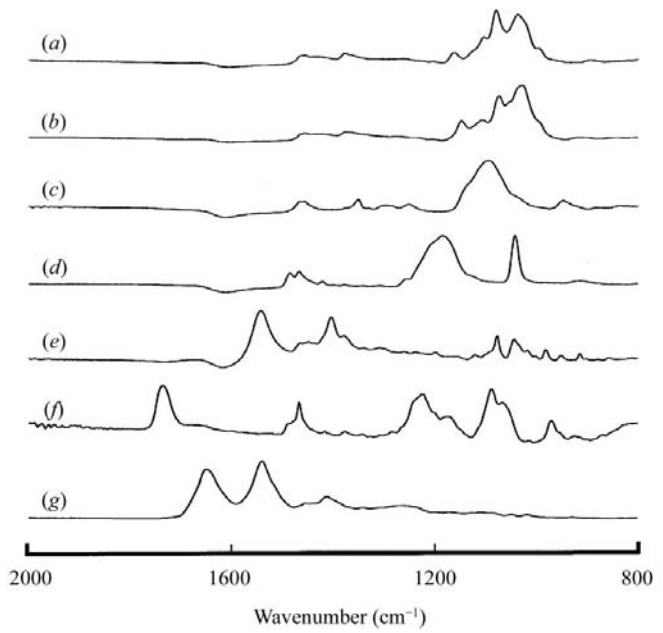

Figure 2
Comparison of ^1H_2O buffer-subtracted FTIR spectra of various detergents with spectra of lipids and protein. (*a*) *n*-Octyl-β-D-glucopyranoside (β-OG), (*b*) *n*-decyl-β-D-maltopyranoside (C_{10}M), (*c*) octaethylene glycol monotridecyl ether ($C_{12}E_8$), (*d*) Zwittergent 3-12, (*e*) cholic acid. Spectrum (*f*) is a dry spectrum of the phospholipid 1,2-dipalmitoyl-*sn*-glycero-3-phosphocholine (DPPC) and spectrum (*g*) is an ^1H_2O-subtracted spectrum of the protein lysozyme.

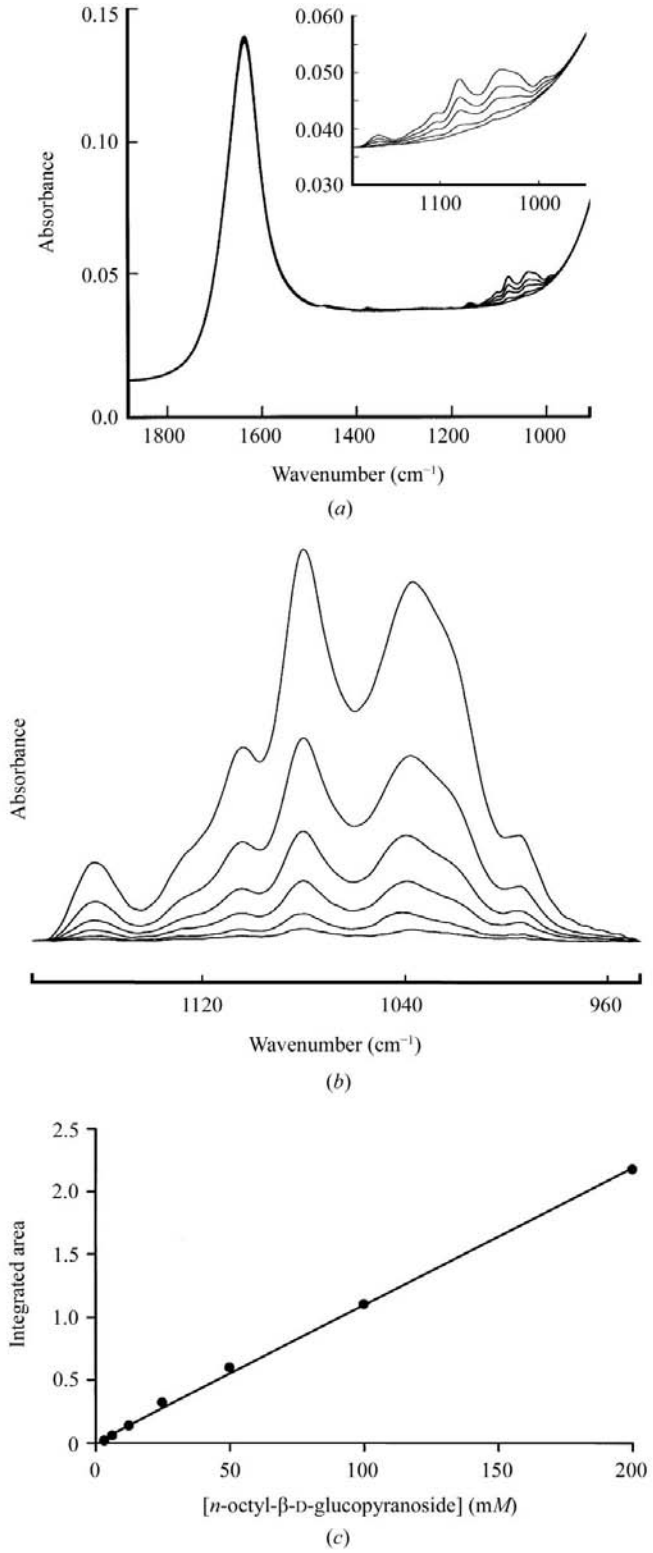

Figure 3
(*a*) Selected aqueous unsubtracted FTIR spectra of various *n*-octyl-β-D-glucoside standards (top trace, 100 m*M* *n*-octyl-β-D-glucoside; bottom trace, 10 m*M* Tris–HCl pH 7.5. (*b*) Aqueous buffer-subtracted FTIR spectra of *n*-octyl-β-D-glucopyranoside standards (baseline-corrected between 1187 and 947 cm^{-1}). The concentration of *n*-octyl-β-D-glucopyranoside in each standard is (from top to bottom): 200, 100, 50, 25, 12.5 and 6.25 m*M*. (*c*) *n*-Octyl-β-D-glucopyranoside standard curve calculated using the spectra in (*b*).

Spectra recorded from solutions with increasing concentrations of the detergent *n*-octyl-β-D-glucoside are presented in Figs. 3(*a*) and 3(*b*). Fig. 3(*a*) shows the intensity of the *n*-octyl-β-D-glucoside peaks relative to the solvent ^1H_2O bending vibration (1640 cm^{-1}) before the buffer is subtracted. Fig. 3(*b*) shows the buffer-subtracted and baseline-corrected spectra used to calculate the standard curve (Fig. 3*c*). The area of the detergent vibrations in the 1200–950 cm^{-1} region correlates in a linear fashion with the concentration of the detergent (Fig. 3*c*), showing that the infrared technique is a viable approach for measuring detergent concentrations in aqueous solutions. Note that accurate spectra of this and other detergents have been recorded to well below their critical micellar concentrations (for octylglucoside this is ∼19–25 m*M*, but for dodecylmaltoside the CMC is only 0.18 m*M*; Le Maire *et al.*, 2000). In fact, accurate infrared spectra have been obtained at detergent concentrations as low as 0.08 m*M* (data not shown). We have found that our concentrated detergent-solubilized membrane-protein samples often exhibit detergent concentrations in the range 10–50 m*M*, which is a highly accurate concentration range for spectral analysis.

It is also important to note that both the shape of the detergent bands and the linearity of their absorption intensities with increasing detergent concentration are unaffected by the CMC. This shows that association of *n*-octyl-β-D-glucoside into micelles does not greatly influence either the shape or intensity of the infrared absorption bands. This result is expected as the absorption bands result from fundamental infrared vibrations, the intensities of which are not dramatically influenced by environmental factors (for example, the infrared absorption bands of acetylcholine are not dramatically changed upon binding to the nAChR even though acetylcholine binds tightly with a nanomolar affinity (Baenziger *et al.*, 1993; other unpublished observations). In addition, the head-group vibrations should have similar hydration states in both the monomeric and micellar forms.

For similar reasons, detergent head-group vibrational bands should not be influenced strongly by the formation of protein–detergent complexes. In support of this assertion, it has been shown that the rate of removal of detergent by dialysis in solubilized N^+/K^+-ATPase samples is equivalent whether monitored using FTIR or radiolabelling techniques (Pistorius *et al.*, 1994).

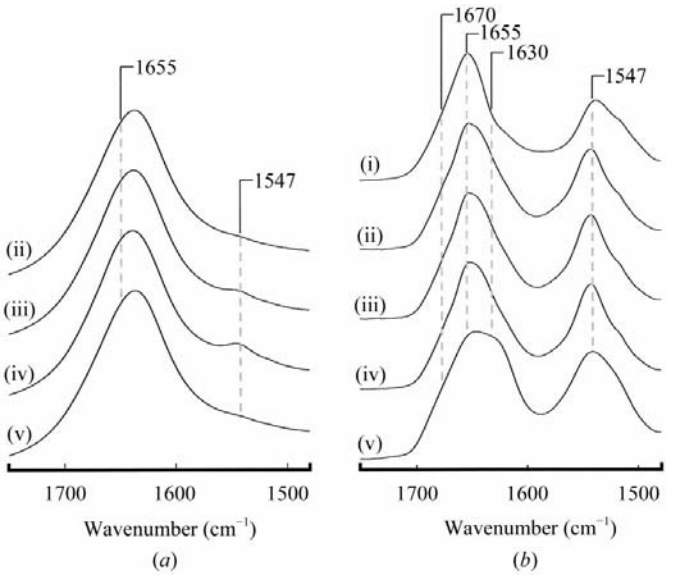

Figure 4
(*a*) Unsubtracted aqueous FTIR spectra of lysozyme. (*b*) Spectra of lysozyme. Spectrum (i), dry lysozyme. Spectra (ii), (iii) and (iv) are ^1H_2O-subtracted spectra of 10, 30 and 60 mg ml^{-1} lysozyme. Spectrum (v) is an ^1H_2O-subtracted spectrum of thermally denatured lysozyme (10 mg ml^{-1}). The spectra in (*b*) have been scaled relative to their amide I band to facilitate band-shape comparison.

3.4. Protein secondary structure

The utility of the diamond ATR accessory for monitoring protein secondary structure was assessed by recording spectra of lysozyme in ^1H_2O. The main difficulty in such an analysis is that the amide I band, which is the vibration whose shape is characteristic of protein secondary structure, overlaps with a strong ^1H_2O vibration in the 1600–1700 cm^{-1} region (see Fig. 4*a*). Analysis of the protein amide I band shape thus requires subtraction of the overlapping ^1H_2O vibration.

Fig. 4 shows spectra recorded from solutions containing 10, 30 and 60 mg ml^{-1} concentrations of lysozyme (spectra ii, iii and iv). In each case, the amide I band shape achieved after subtraction of the overlapping ^1H_2O vibration (Fig. 4*b*) is similar to that obtained in a spectrum of lysozyme dried on the ATR accessory (Fig. 4*b*, spectrum i). Specifically, each amide I band exhibits an intense maximum near 1655 cm^{-1}, characteristic of α-helical secondary structure, and less intense shoulders near 1630 and 1670 cm^{-1}, characteristic of β-sheet (Jackson & Mantsch, 1995). As expected, all four spectra are indicative of a predominantly α-helical protein with substantial β-sheet.

In contrast, the amide I band shapes differ substantially from that observed in a spectrum recorded from lysozyme after thermal denaturation (Fig. 4, spectrum v). Upon denaturation, the amide I band exhibits an increase in intensity at both 1620 and 1680 cm^{-1}, features that are observed in the spectra of numerous denatured proteins (Methot & Baenziger, 1998; Young *et al.*, 1995). Similar, although less pronounced, changes in amide I band shape have also been detected in spectra of lysozyme and the nicotinic acetylcholine receptor (nAChR) recorded in the presence of high concentrations of detergent (data not shown), although subtle changes in the amide I band shape can be difficult to detect owing to the subjectivity involved in the subtraction of the overlapping water vibration. We have found that FTIR can provide a qualitative estimate of the structural stability of a membrane protein in the presence of detergent. A more definitive analysis can be performed by recording spectra in ^2H_2O buffer, as ^2H_2O does not exhibit vibrations overlapping the 1600–1700 cm^{-1} region (He *et al.*, 1991). In addition, spectra can be obtained after drying the sample on the ATR surface to eliminate the ^1H_2O vibrations in the spectra. It should be noted, however, that drying concentrates the

detergent in the sample, which could result in protein denaturation.

3.5. Changes in detergent levels during sample manipulations

To demonstrate the utility of the ATR technique for monitoring detergent levels during the preparation of a membrane-protein stock solution that is suitable for crystallization trials, we examined the changes in detergent levels that occur during concentration of affinity-purified nAChR. The nAChR was first solubilized from its native membranes and affinity purified in the presence of the detergent cholate. The cholate-solubilized nAChR was then concentrated by ultrafiltration in an Amicon protein concentrator (100 kDa MWCO).

Protein assays show that there is a very slow increase in protein concentration during the first 35 min of the spin, but thereafter the protein concentration increases at a dramatic rate. In contrast, the detergent concentration increases only slightly during the first 50 min of the spin (Fig. 5). We believe that the lag time between the increases in detergent and protein concentration may be because of the fact that excess protein-free detergent micelles exist in solution and initially spin through the 100 kDa MWCO Amicon filters. When the detergent is no longer in excess, it concentrates at the same rate as the protein because they are tightly associated.

Using our FTIR techniques, we have found that the initial lipid:protein ratio in our nAChR samples can influence the degree to which the detergent concentrates during protein concentration. This may occur because excess lipid forms protein free lipid–detergent mixed micelles that may be too large to spin through the 100 kDa MWCO filters.

In addition, properties of the detergent (*i.e.* micellar size) as well as the size of the filter pores may influence how much the detergent concentrates. With ultrafiltration devices that have a MWCO that is large enough to allow the free passage of detergent micelles, the concentration of detergent monomers and micelles stays the same over the course of a typical concentration experiment, while the ratio of micelles and monomers to protein–detergent complexes (PDCs) decreases (Fig. 6). Therefore, it is best to minimize the initial amount of excess detergent in a solubilized membrane-protein sample before ultrafiltration.

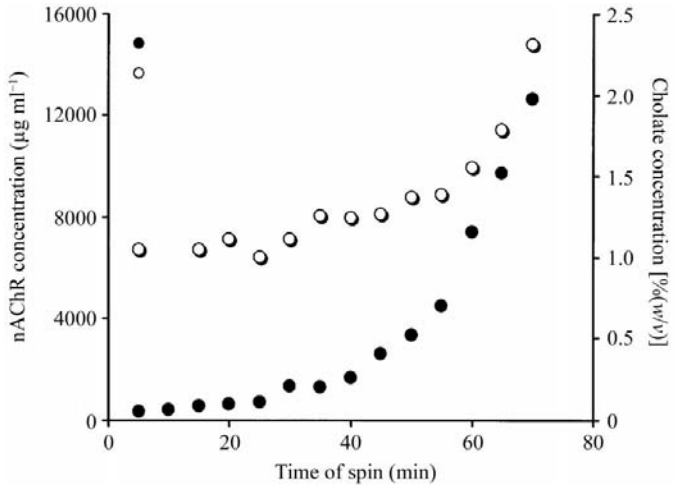

Figure 5
A comparison of how detergent and protein concentration change during the concentration of cholate-solubilized nAChR by ultrafiltration. Solid circles correspond to [nAChR]. Open circles correspond to [cholate].

4. Discussion

The goal of this work was to develop a rapid and effective spectroscopic method for monitoring lipid:protein ratios and detergent concentrations in detergent-solubilized membrane protein samples. The rationale for developing this technique stems from the fact that every membrane protein likely has a limited range of both lipid:protein and detergent:protein ratios where the protein remains both structurally intact and soluble as a monomer in solution. In order to prepare solubilized membrane-protein samples that are ideal for crystallization, one must establish how lipid:protein and detergent:protein ratios influence both stability and solubility. To develop effective purification protocols, it is important to know how common sample manipulations, such as protein dialysis and concentration *etc.* influence lipid:protein and detergent:protein ratios. The ability to assess lipid:protein and detergent:protein ratios in final protein stock solutions is also advantageous to ensure reproducibility and aid in the interpretation of crystallization screens.

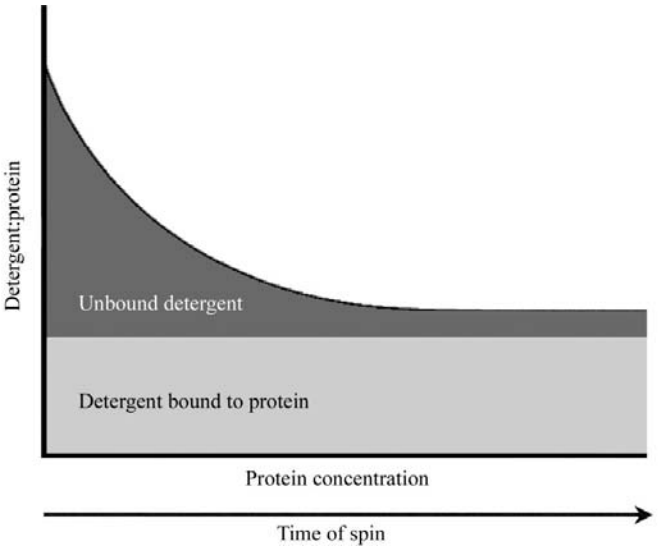

Figure 6
Conceptual depiction of how detergent:protein ratios vary with protein concentration during an ultrafiltration experiment. At the start of the experiment, there is a low protein concentration and excess detergent is present as protein-free micelles. If the molecular-weight cutoff of the protein concentrator is large, the micelles spin through the filter of the concentrator and do not concentrate during the experiment. Although the absolute concentration of micelles and monomers does not change, their molar ratio relative to protein–detergent complexes decreases. Therefore, the final ratio of protein-free detergent micelles and monomers to protein–detergent complexes depends on both the starting concentration of the detergent and the final concentration of protein. Initial detergent concentrations close to the critical micellar concentration of the detergent are likely to be ideal.

We show here that the diamond ATR sampling accessory can be used to record FTIR spectra from 10 µl aliquots of solution. These FTIR spectra can be analyzed to determine both the lipid:protein ratio and the detergent concentration in a detergent-solubilized membrane-protein sample. The lipid:protein ratios are accurate down to a level of five molecules of lipid per molecule of 300 kDa protein. The detergent concentrations are accurate to well below the CMCs of common detergents used in crystallization trials. The FTIR spectra can also be used to qualitatively assess the effects of detergent on protein structural stability.

The advantages of this FTIR approach include its rapidity and accuracy. Multiple small aliquots can be analyzed in a short period of time. In contrast, using thin-layer chromatography to measure lipid:protein ratios is qualitative (Garavito & Picot, 1990) and the use of radiolabelled detergents to measure detergent concentrations (Le Maire *et al.*, 1983) is a time-consuming and expensive proposition. The ability to rapidly measure both lipid:protein and detergent:protein ratios should aid in the rapid development of protocols for the stable solubilization and purification of any membrane protein and will thus help open the bottleneck in membrane-protein crystallization.

References

Baenziger, J. E., Miller, K. W. & Rothschild, K. J. (1993). *Biochemistry*, **32**, 5448–5454.

daCosta, C. J., Ogrel, A. A., McCardy, E. A., Blanton, M. P. & Baenziger, J. E. (2002). *J. Biol. Chem.* **277**, 201–208.

Garavito, R. M. & Picot, D. (1990). *Methods*, **1**, 57–69.

Garavito, R. M., Picot, D. & Loll, P. J. (1996). *J. Bioenerg. Biomembr.* **28**, 13–27.

Garavito, R. M. & Rosenbusch, J. P. (1986). *Methods Enzymol.* **125**, 309–328.

Goormaghtigh, E., Cabiaux, V. & Ruysschaert, J. M. (1990). *Eur. J. Biochem.* **193**, 409–420.

He, W. Z., Newell, W. R., Haris, P. I., Chapman, D. & Barber, J. (1991). *Biochemistry*, **30**, 4552–4559.

Hitscherich, C. Jr, Kaplan, J., Allaman, M., Wiencek, J. & Loll, P. J. (2000). *Protein Sci.* **9**, 1559–1566.

Jackson, M. & Mantsch, H. H. (1995). *Crit. Rev. Biochem. Mol. Biol.* **30**, 95–120.

Kuhlbrandt, W. (1988). *Q. Rev. Biophys.* **21**, 429–477.

Le Maire, M., Champeil, P. & Moller, J. V. (2000). *Biochim. Biophys. Acta*, **1508**, 86–111.

Le Maire, M., Kwee, S., Andersen, J. P. & Moller, J. V. (1983). *Eur. J. Biochem.* **129**, 525–532.

Loll, P. J., Allaman, M. & Wiencek, J. (2001). *J. Cryst. Growth*, **232**, 432–438.

Mendelsohn, R. & Mantsch, H. H. (1986). *Protein–Lipid Interactions 2*, edited by W. D. Pont, pp. 103–224. Amsterdam: Elsevier Science Publishers BV.

Methot, N. & Baenziger, J. E. (1998). *Biochemistry*, **37**, 14815–14822.

Ostermeier, C. & Michel, H. (1997). *Curr. Opin. Struct. Biol.* **7**, 697–701.

Pebay-Peyroula, E., Garavito, R. M., Rosenbusch, J. P., Zulauf, M. & Timmins, P. A. (1995). *Structure*, **3**, 1051–1059.

Pistorius, A. M., Stekhoven, F. M., Bovee-Geurts, P. H. & de Grip, W. J. (1994). *Anal. Biochem.* **221**, 48–52.

Reid, S. E., Moffat, D. J. & Baenziger, J. E. (1996). *Spectrochim. Acta A*, **52**, 1347–1356.

Rosenbusch, J. P., Lustig, A., Grabo, M., Zulauf, M. & Regenass, M. (2001). *Micron*, **32**, 75–90.

Roth, M., Lewit-Bentley, A., Michel, H., Deisenhofer, J., Huber, R. & Oesterhelt, D. (1989). *Nature (London)*, **340**, 659–662.

Young, N. M., MacKenzie, C. R., Narang, S. A., Oomen, R. P. & Baenziger, J. E. (1995). *FEBS Lett.* **377**, 135–139.